

**Praca wykonana w ramach projektu TEAM  
kierowanego przez Prof. Pawła Moskala. Projekt  
finansowany przez Fundację na rzecz Nauki Polskiej.**



**Jagiellonian University in Kraków**

Faculty of Physics, Astronomy and Applied Computer Science

**Agata Jędruszczak**

Student's number: 1153045

**Simulations of absorption in the brain  
of gamma quanta from positronium atoms**

Bachelor Thesis in physics

Supervised by  
Prof. dr hab. Paweł Moskal  
Department of Experimental  
Particle Physics and Applications

Kraków 2021

## **Acknowledgments**

This thesis was performed in the framework of the TEAM POIR.04.04.00-00-4204/17 program funded by the Foundation for Polish Science.

I would like to thank prof. dr hab. P. Moskal for the opportunity to participate in the TEAM program and the J-PET group, and for his patience and valuable advice while writing this thesis.

## Abstract

Positronium imaging is a new method that can be used for PET scanning. This method allows not only to determine the location of the tumor, but also to analyze the structure of the tissue. What is important is how many gamma quanta from a positronium atom reach the detector. The main goal of this work is to study the absorption in the brain of gamma quanta from a positronium atom. The brain in this study is approximated by a sphere with water. The  $3\gamma/2\gamma$  ratio, a parameter that reflects the tissue structure, is determined. For this purpose, Monte Carlo simulations of positron decays into  $2\gamma$  and  $3\gamma$  and photon absorption in the brain and skull were performed. The simulation results were compared with theoretical calculations. The results of the percent events for which none of photons scattered in the head are as follows:  $26.10 \pm 0.05$  % for para-positronium and  $8.40 \pm 0.03$  % for ortho-positronium (absorption in the brain),  $20.84 \pm 0.05$  % for para-positronium,  $5.46 \pm 0.02$  % for ortho-positronium (absorption in the brain and in skull). The values of the  $3\gamma/2\gamma$  ratio from the simulation are:  $0.322 \pm 0.002$  for absorption in the brain and  $0.262 \pm 0.002$  for absorption in the brain and skull. The dependence of absorption probability of photons in the head on the location of positronium atom decay in the brain is determined.

## Streszczenie

Obrazowanie pozytonium jest nową metodą, którą można wykorzystać do badania PET. Metoda ta pozwala nie tylko na określenie lokalizacji miejsca nowotworu, ale również na analizę struktury tkanki. Istotne jest to, ile kwantów gamma wydostaje się z ciała pacjenta i dociera do detektora, w związku z tym głównym celem tej pracy jest zbadanie absorpcji w ciele pacjenta kwantów gamma pochodzących z rozpadu atomu pozytonium. W tej pracy rozważono absorpcję fotonów w mózgu, który został przybliżony sferą z wody. Wyznaczono stosunek  $3\gamma/2\gamma$ , czyli parametr informujący o strukturze tkanki. W tym celu przeprowadzono symulacje Monte Carlo rozpadów atomu pozytonium na  $2\gamma$  i  $3\gamma$  oraz absorpcji fotonów w mózgu i czaszce. Wyniki symulacji zostały porównane z obliczeniami teoretycznymi. Wyniki procentowe zdarzeń, dla których żaden foton nie uległ rozproszeniu w głowie są następujące:  $26,10 \pm 0,05$  % dla para-pozytonium i  $8,40 \pm 0,03$  % dla orto-pozytonium (absorpcja w mózgu),  $20,84 \pm 0,05$  % dla para-pozytonium,  $5,46 \pm 0,02$  % dla orto-pozytonium (absorpcja w mózgu i w czaszce). Wartości stosunku  $3\gamma/2\gamma$  z symulacji wynoszą:  $0,322 \pm 0,002$  dla absorpcji w mózgu i  $0,262 \pm 0,002$  dla absorpcji w mózgu i czaszce. Określono zależność prawdopodobieństwa pochłonięcia fotonów w głowie od miejsca rozpadu atomu pozytonium w mózgu.

# Contents

List of Figures	IV
List of Tables	V
<b>1 Introduction</b>	<b>1</b>
<b>2 Positronium imaging</b>	<b>3</b>
<b>3 Positronium decay</b>	<b>4</b>
3.1 Para-positronium . . . . .	4
3.2 Ortho-positronium . . . . .	4
<b>4 Interaction of gamma quanta with matter</b>	<b>10</b>
<b>5 Gamma quantum absorption for annihilation at the center of the brain</b>	<b>12</b>
5.1 Results . . . . .	13
<b>6 Gamma quantum absorption for annihilation in a random place in the brain</b>	<b>20</b>
<b>7 <math>3\gamma/2\gamma</math> ratio</b>	<b>26</b>
7.1 Annihilation is at the center of the brain . . . . .	26
7.2 Dependence of the ratio $3\gamma/2\gamma$ on the location of the decay . . . . .	26
<b>8 Summary</b>	<b>28</b>

# List of Figures

Figure 1:	Scheme of annihilation in the brain, blue circle denotes brain, beige circle denotes skull, red point is a place of decay, arrows denote photons, grey, dashed circle denotes detector. . . . .	2
Figure 2:	Image of positronium atom - rotating electron and positron. . . . .	4
Figure 3:	Image of para-positronium. . . . .	4
Figure 4:	Image of ortho-positronium. . . . .	5
Figure 5:	Energy spectrum of gamma quanta from ortho-positronium decay. . .	7
Figure 6:	Dalitz plots - distribution of energy of ortho-positronium decay. . . .	8
Figure 7:	Distribution of relate angles between photons from ortho-positronium decay. . . . .	9
Figure 8:	Linear attenuation coefficient for water with cubic interpolation. . . .	11
Figure 9:	Linear attenuation coefficient for bones with linear interpolation. . . .	11
Figure 10:	Distribution of energy of gamma quanta from ortho-positronium decay after passing through the brain. . . . .	16
Figure 11:	Distribution of the ratio of gamma quanta from ortho-positronium decay after passing through the brain (Figure 10) and distribution of energy of all gamma quanta from ortho-positronium decay (Figure 6). . . . .	17
Figure 12:	Distribution of energy of gamma quanta from ortho-positronium decay after passing through the brain and skull. . . . .	18
Figure 13:	Distribution of the ratio of gamma quanta from ortho-positronium decay after passing through the brain (Figure 12) and distribution of energy of all gamma quanta from ortho-positronium decay (Figure 6). . . . .	19
Figure 14:	Homogeneous distribution of points in the sphere. . . . .	21
Figure 15:	$d_1, d_2$ are the distances in the brain, $d'_1, d'_2$ are the distances in the skull. . . . .	22
Figure 16:	Dependence of percent of events with non-absorbed photons on place of annihilation (distance $d_o$ from the center of the brain to point $\vec{o}$ ). Case: para-positronium and brain. . . . .	23
Figure 17:	Dependence of percent of events with non-absorbed photons on place of annihilation (distance $d_o$ from the center of the brain to point $\vec{o}$ ). Case: ortho-positronium and brain. . . . .	24
Figure 18:	Dependence of percent of events with non-absorbed photons on place of annihilation (distance $d_o$ from the center of the brain to point $\vec{o}$ ). Case: para-positronium and brain with skull. . . . .	24
Figure 19:	Dependence of percent of events with non-absorbed photons on place of annihilation (distance $d_o$ from the center of the brain to point $\vec{o}$ ). Case: ortho-positronium and brain with skull. . . . .	25

Figure 20:	Dependence of the $3\gamma/2\gamma$ ratio on place of annihilation (distance $d_o$ from the center of the brain to point $\vec{o}$ ). Case: brain. . . . .	27
Figure 21:	Dependence of the $3\gamma/2\gamma$ ratio on place of annihilation (distance $d_o$ from the center of the brain to point $\vec{o}$ ). Case: brain with skull. . . . .	27

## List of Tables

Table 1:	Formulas for total probabilities for non-physical cases. . . . .	13
Table 2:	Fraction of non-absorbed gamma quanta for the different scattering. Case: para-positronium and brain. . . . .	15
Table 3:	Fraction of non-absorbed gamma quanta for the different scattering. Case: ortho-positronium and brain. . . . .	15
Table 4:	Fraction of non-absorbed gamma quanta for the different scattering. Case: para-positronium and brain with skull. . . . .	15
Table 5:	Fraction of non-absorbed gamma quanta for the different scattering. Case: ortho-positronium and brain with skull. . . . .	15
Table 6:	$3\gamma/2\gamma$ ratio for Monte Carlo and Analytical calculations for two cases: brain and brain with skull. . . . .	26

# 1 Introduction

Positronium imaging is a new imaging method that allows to determine not only the location of the tumor, but also the degree of its expansion [1]. It is the multi-photon imaging, which uses not only  $2\gamma$ , but also  $3\gamma$  to annihilations. Amount of detected photons from decay into  $2\gamma$  or  $3\gamma$  give information about tissue structure. Moreover, the  $3\gamma/2\gamma$  ratio allows the description of neoplastic changes [2]. Hence, the purpose of this thesis is to determine how many gamma quanta from positronium atoms are not absorbed in the brain and skull and be able to get to the detector and, in the end, can be used for determination of the  $3\gamma/2\gamma$  ratio.

According to data collected in 2018 by GLOBOCAN, 296,851 cases of brain and nervous system cancer were diagnosed worldwide, which accounted for 1.6% of all cancer cases. The death rate was equal to 241,037, accounting for 2.5% of all cancer deaths [3]. The main method to diagnose brain cancer are magnetic resonance imaging (MRI) and computed tomography (CT), but the future in imaging neoplastic changes may be positron emission tomography (PET). The advantage of this method is the ability to observe the biological aspects of the tumor [2]. In a typical PET scan, the density distribution of the radiopharmaceutical in the patient's body is obtained, which enables localization of the tumor site. The radiopharmaceutical accumulates at the tumor site, where  $\beta^+$  decay then takes place. Positrons are emitted (from  $\beta^+$  decay), which then annihilate, resulting in the formation of two gamma quanta. Photons are registered by a detector and thanks to them it is possible to determine the place of annihilation, which reveals the location of neoplastic changes [2]. Sometimes, in the patient body, before the positron is annihilated with the electron, the positron loses energy and then forms a positronium atom with the electron. Positronium can decay into two or three gamma quanta. The relative fraction of these decays depends on the structure of the tissue. Thus, a new parameter can be defined which, by registering gamma quanta in the detector, will give information about the neoplastic characters, not only about the tumor site. This parameter is  $3\gamma/2\gamma$  ratio [2]. To determine it a multi-photon imaging is required, which is currently being developed in J-PET [1].

When positronium atoms are in the brain some of gamma quanta from decay are absorbed in the brain and in the skull. Photons that are not absorbed can be detected by detectors to determine the location of the tumor and the  $3\gamma/2\gamma$  ratio. The number of events detected in typical PET scan is  $10^6 - 10^9$ . The purpose of this work is to find out how many gamma quanta from positronium decay in the brain will pass through the head and be able to arrive to the detector. Simulations were carried out using ROOT program. In this study brain is approximated by the sphere with water and the basis case of simulations is decay of positronium in the center of the brain. Then I consider that the gamma quanta also pass through the skull. This case is illustrated in the scheme shown in Figure 1.

Simulations of positronium decay is described in chapter 3. Details relating to the attenuation coefficient are described in chapter 4, absorption of gamma quanta in the brain and results are described in chapter 5. In chapter 6 absorption of photons as a function of the distance in the brain is discussed. Chapter 7 presents results of  $3\gamma/2\gamma$  ratio for central position of tumor and dependence of ratio on the location of the decay.

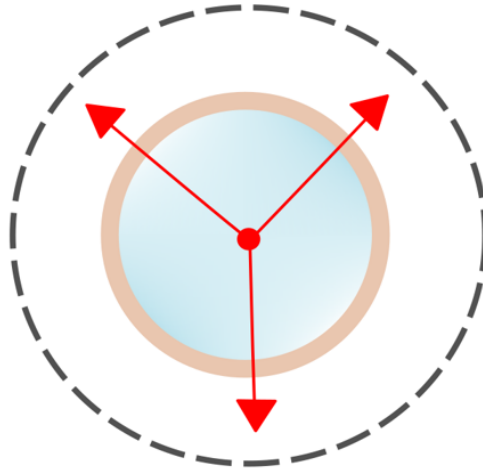


**Figure 1:** Scheme of annihilation in the brain, blue circle denotes brain, beige circle denotes skull, red point is a place of decay, arrows denote photons, grey, dashed circle denotes detector.

## 2 Positronium imaging

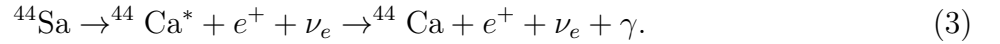
The basis of PET scanning is  $\beta^+$  decay as a result of which positron  $e^+$  (electron  $e^-$  antiparticle) is emitted:



where  $\nu_e$  is electron neutrino. Positron annihilates with electron from patient body and create predominantly two or three photons:



Current PET uses only  $2\gamma$  for imaging and  $3\gamma$  is a source of background [1].  $2\gamma$  imaging allows to check the density distribution of radiopharmaceutical in the patient's body, thus determining the location of the cancer. The new method used in J-PET allows to employ  $3\gamma$  for reconstruction [1]. This option is very handy because in 40 % cases when positron meets electron they create a positronium atom and 30 % is ortho-positronium (o-Ps), which decays into  $3\gamma$ . Other 10 % is para-positronium (p-Ps), which decays into  $2\gamma$  [4]. Ortho-positronium is long-lived atom (142 ns) and para-positronium is short-lived (125 ps) [5], [6]. As opposed to a standard PET scan, which uses radiopharmaceuticals containing beta-plus isotopes such as fluorine  ${}^{18}\text{F}$ , positronium imaging uses beta-plus isotopes, which then emit prompt gamma  $\gamma$ . Such an isotope is for example scandium  ${}^{44}\text{Sc}$ , whose decay chain is as follows [4]:



Prompt gamma  $\gamma$  is used for measurement of time of positronium formation and, that together with the time from annihilation, allows to determine a lifetime of positronium [4]. Multi-photon imaging allows to designate how many decays produce  $2\gamma$  and how many  $3\gamma$ . From this possibility, a new parameter can be defined, which is expressed by the  $3\gamma/2\gamma$  ratio. This ratio can help staging a tumor, because it gives information about tissue porosity and cell abnormalities [2]. Ortho-positronium lifetime strongly depends on free space between atoms in tissues. Hence the amount of  $3\gamma$  quanta is correlated to the structure of the tissue. Thus,  $3\gamma/2\gamma$  ratio can give information about tissue deformation which can describe neoplastic changes.

### 3 Positronium decay

Positronium is formed by electron and positron, which rotate around a common center of mass creating hydrogen-like system. Positronium atom has two state because of spin: para-positronium (spin equal to 0) and ortho-positronium (spin equal to 1) [7].

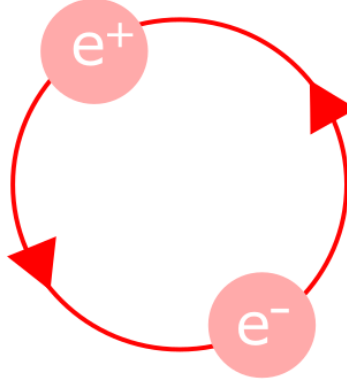


**Figure 2:** Image of positronium atom - rotating electron and positron.

#### 3.1 Para-positronium

Para-positronium is in the singlet state  $^1S_0$ , because total spin is equal to 0. It decays into  $2\gamma$ . Both of created  $\gamma$  quanta has the same energy  $E = 511$  keV. The angle between the  $\gamma$  quanta is  $180^\circ$ .



**Figure 3:** Image of para-positronium.

#### 3.2 Ortho-positronium

Ortho-positronium is in triplet state  $^3S_1$ , because the total spin is equal to 1. It decays into  $3\gamma$ . This decay is defined by matrix element  $M_{oPs \rightarrow 3\gamma}$  provided by QED.  $M_{oPs \rightarrow 3\gamma}$  is Lorentz invariant and contains information about the dynamics [7]:

$$M_{oPs \rightarrow 3\gamma} = \left( \frac{m_e - E_1}{E_2 E_3} \right)^2 + \left( \frac{m_e - E_2}{E_1 E_3} \right)^2 + \left( \frac{m_e - E_3}{E_1 E_2} \right)^2, \quad (4)$$

where  $m_e$  is electron mass,  $E_1, E_2, E_3$  are energies of gamma quanta.

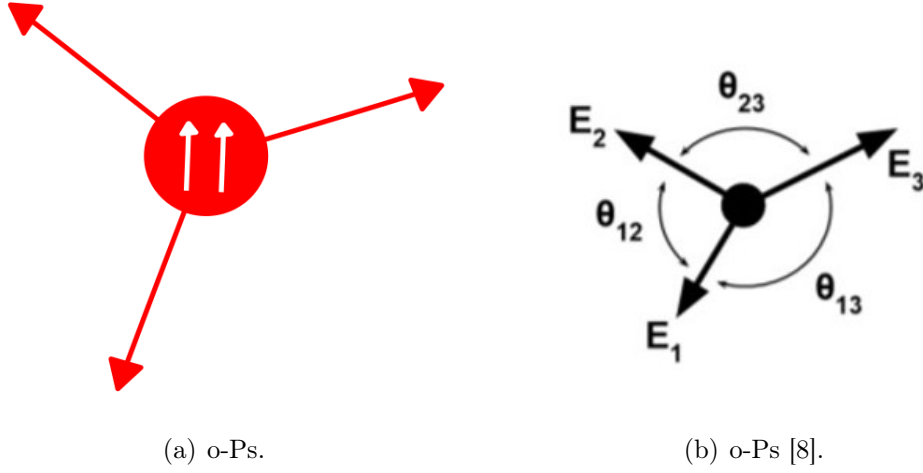


**Figure 4:** Image of ortho-positronium.

From momentum-energy conservation follows relations between energies  $E_i$  of photons and angles between them  $\theta_{ij}$ , where  $i, j = 1, 2, 3$  [8]:

$$E_1 = \frac{-2m_e(\cos \theta_{31} + \cos \theta_{12} \cos \theta_{23})}{(1 + \cos \theta_{12})(1 + \cos \theta_{12}) - \cos \theta_{23} \cos \theta_{21}}, \quad (5)$$

$$E_2 = \frac{-2m_e(\cos \theta_{23} + \cos \theta_{12} \cos \theta_{31})}{(1 + \cos \theta_{12})(1 + \cos \theta_{12}) - \cos \theta_{23} \cos \theta_{31}}, \quad (6)$$

$$E_3 = \frac{-2m_e(1 + \cos \theta_{12})}{(1 + \cos \theta_{12} - \cos \theta_{23}) \cos \theta_{31}}, \quad (7)$$

and relations between momentum  $p_i$  and angles  $\theta_{ij}$  [9]:

$$\theta_{12} = \cos^{-1} \left( \frac{p_3^2 - p_1^2 - p_2^2}{2p_1 p_2} \right), \quad (8)$$

$$\theta_{23} = \cos^{-1} \left( \frac{p_1^2 - p_2^2 - p_3^2}{2p_2 p_3} \right), \quad (9)$$

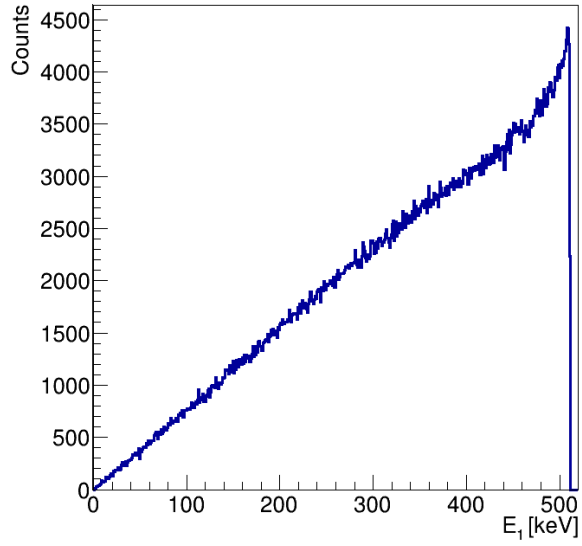
$$\theta_{31} = \cos^{-1} \left( \frac{p_2^2 - p_1^2 - p_3^2}{2p_1 p_3} \right). \quad (10)$$

I simulate o-Ps decay by using Monte Carlo method. Firstly I define matrix element from equation 4 and Lorentz vector  $w$  for positronium:

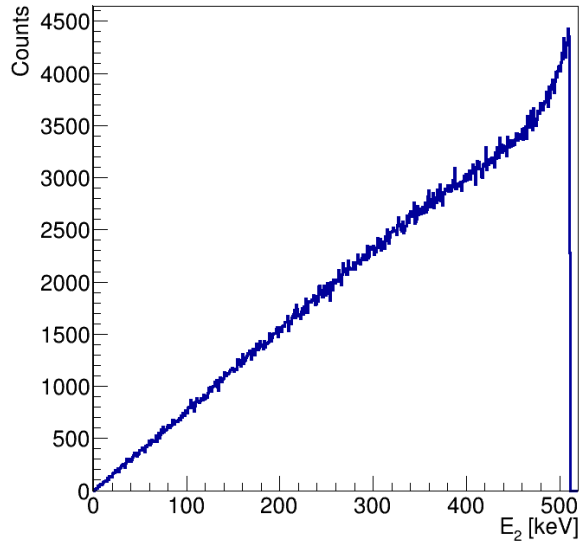
$$w = (0.0, 0.0, 0.0, 1022), \quad (11)$$

where first three number in vector are momentum of positronium. They are equal to 0, because positronium is at rest. Fourth number is energy  $E = 1022$  keV. For defining this vector I use function from ROOT `TLorentzVector()`. I define gamma quanta masses after decay, they are equal to zero. To generate event I use variable from *TGenPhaseSpace* and *Get.Decay()* function. Then I use Monte Carlo hit and miss method with the weight specified by the matrix element from equation 4. As a result of this draw I get Lorentz vector for each gamma quantum with momentum vectors  $(p_1, p_2, p_3)$  and energies  $(E_1, E_2, E_3)$ . Energies distributions are present in Figure 5, Dalitz plot energy distributions are shown in Figure 6. From momentum vectors I can calculate angles between photons using equations 8, 9, 10. Angle distribution is shown in Figure 7. Momentum vectors define photons directions after decay.

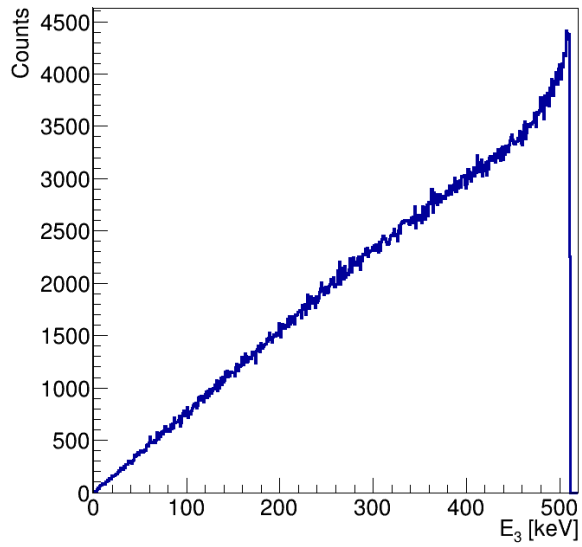
For para-positronium I generate events with two gamma quanta from p-Ps decay with energy equal to  $E = 511$  keV. Para-positronium decays isotropically, so gamma quanta direction after decay can be randomly selected in homogenous sphere. The method of selecting the unit vector  $\vec{u}$  that determines the direction of photons is described in chapter 6.



(a) Energy spectrum of first gamma quanta ( $E_1$ ).

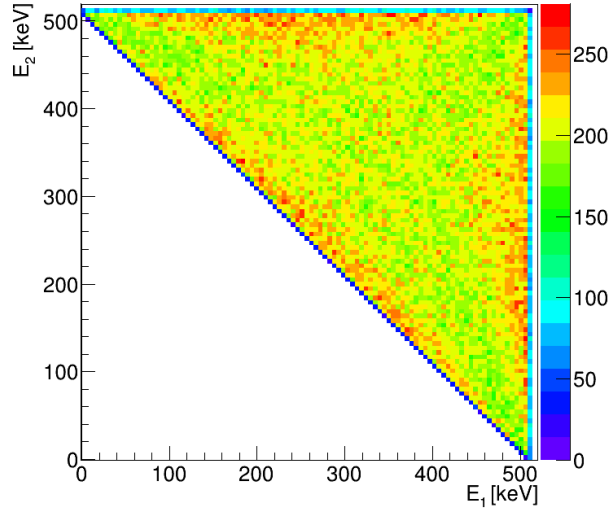


(b) Energy spectrum of second gamma quanta ( $E_2$ ).

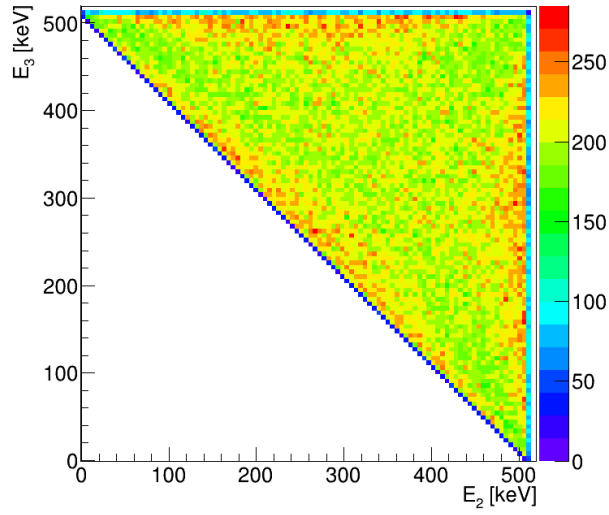


(c) Energy spectrum of third gamma quanta ( $E_3$ ).

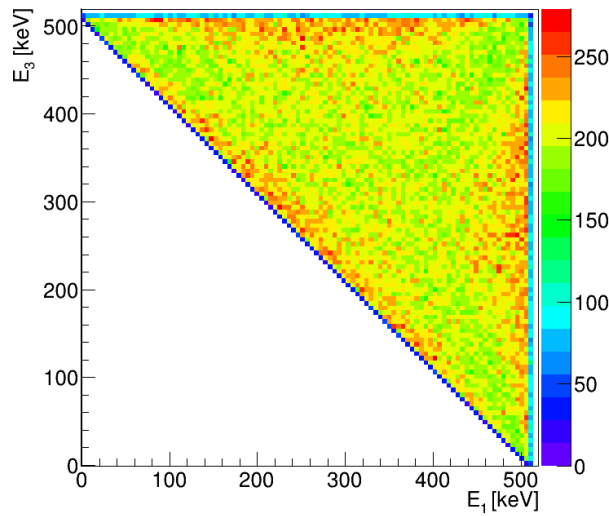
**Figure 5:** Energy spectrum of gamma quanta from ortho-positronium decay.



(a) Distribution of  $E_1$  and  $E_2$ .

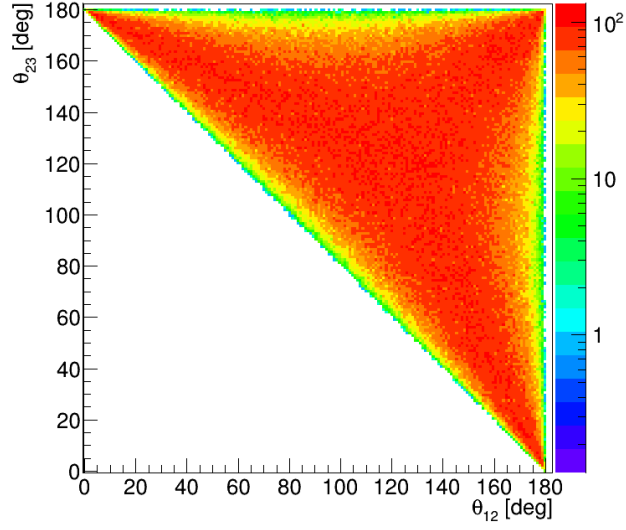


(b) Distribution of  $E_2$  and  $E_3$ .

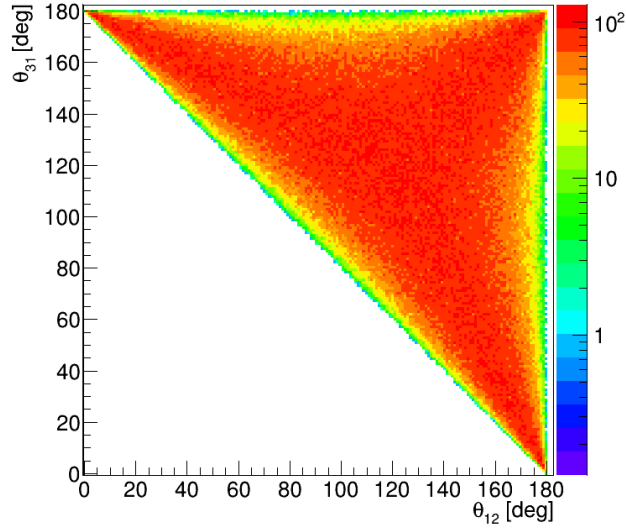


(c) Distribution of  $E_1$  and  $E_3$ .

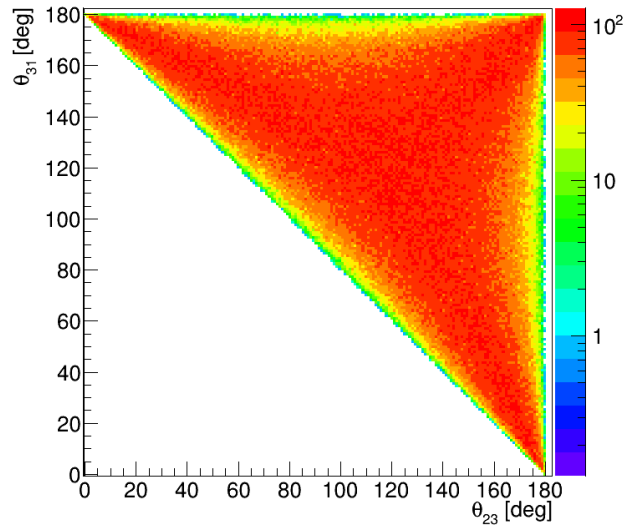
**Figure 6:** Dalitz plots - distribution of energy of ortho-positronium decay.



(a) Distribution of  $\theta_{12}$  and  $\theta_{23}$ .



(b) Distribution of  $\theta_{12}$  and  $\theta_{31}$ .



(c) Distribution of  $\theta_{31}$  and  $\theta_{23}$ .

**Figure 7:** Distribution of relate angles between photons from ortho-positronium decay.

## 4 Interaction of gamma quanta with matter

Photons after decay can be absorbed in the brain and skull. How many gamma quanta can be absorbed is given by exponential function and depends on linear attenuation coefficient  $\mu$  and distance  $d$  [10]:

$$N = N_0 e^{-\mu d}, \quad (12)$$

where  $N$  is number of photons which went through the material,  $N_0$  is initial number of photons. The main cause of the absorption of gamma radiation are three phenomena: photoelectric effect, Compton scattering and pair production. Cross-section for each phenomena depends on energy and total absorption cross-section is equal to the sum of the cross-sections for the above phenomena. In the studies presented in this thesis brain is approximated by sphere with water, so absorption gamma quanta in the brain depends on linear attenuation coefficient for water. I generated values of mass attenuation coefficient  $\mu_{mass}$  as a function of energy using software from reference [11]. Attenuation coefficient for skull is approximately mass coefficient for bones from tables [12]. For calculation of absorption a linear attenuation coefficient  $\mu$  is needed. Relation between those two coefficients is equal:

$$\mu = \rho \mu_{mass}, \quad (13)$$

where  $\rho$  is material density. Hence brain and skull densities are needed to calculate linear attenuation coefficients. Water density in temperature  $26.7^\circ$  is equal [13]:

$$\rho_{water} = 0.997 \frac{\text{g}}{\text{cm}^3}, \quad (14)$$

bones density [12]:

$$\rho_{bones} = 1.92 \frac{\text{g}}{\text{cm}^3}. \quad (15)$$

The data in references [11], [12] are only for finite number of energy values, but there may be many different energies from the decay of o-Ps and for each energy an attenuation coefficient is needed for simulation. For this purpose, using reference data, I do interpolation: cubic for water (Figure 8), linear for bones (Figure 9). Cubic interpolation rely on fitting 3-degree polynomial to points  $x_{i-2}$ ,  $x_{i-1}$  and  $x_i$ . In simulation it is performed by function *TSpline3()*. Linear interpolation fit linear function to points  $x_{i-1}$  and  $x_i$ . Plots from data and interpolation is shown in Figures 8, 9. Value of linear attenuation coefficient for photon energy  $E = 511$  keV calculated by interpolation is:

$$\mu = 0.096 \frac{1}{\text{cm}} \quad \text{for water}, \quad (16)$$

$$\mu = 0.172 \frac{1}{\text{cm}} \quad \text{for bone}. \quad (17)$$

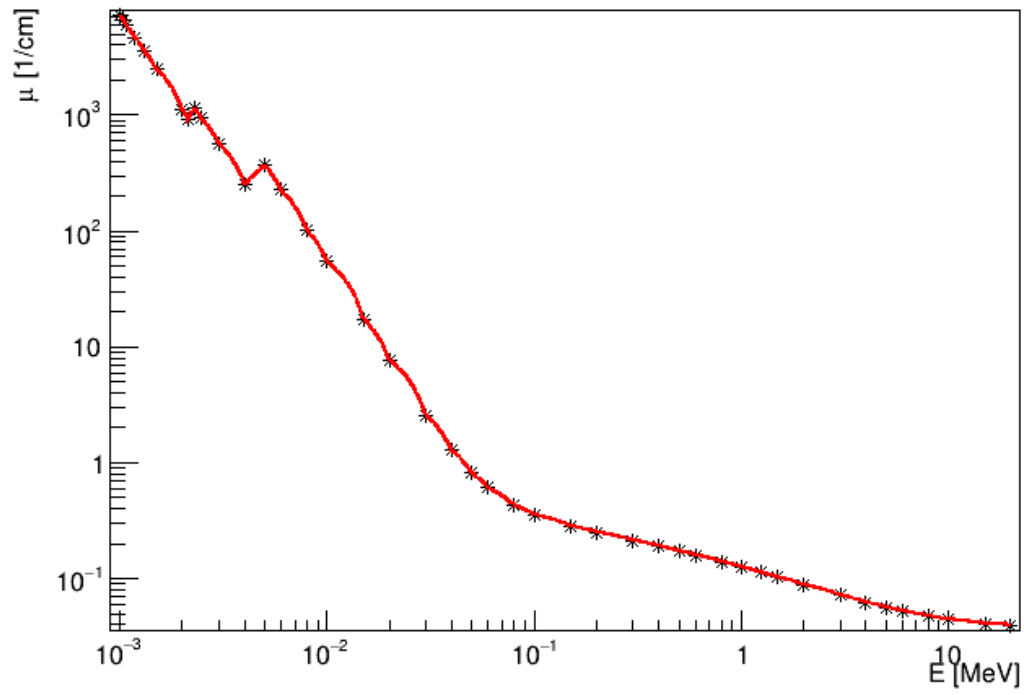


Figure 8: Linear attenuation coefficient for water with cubic interpolation.

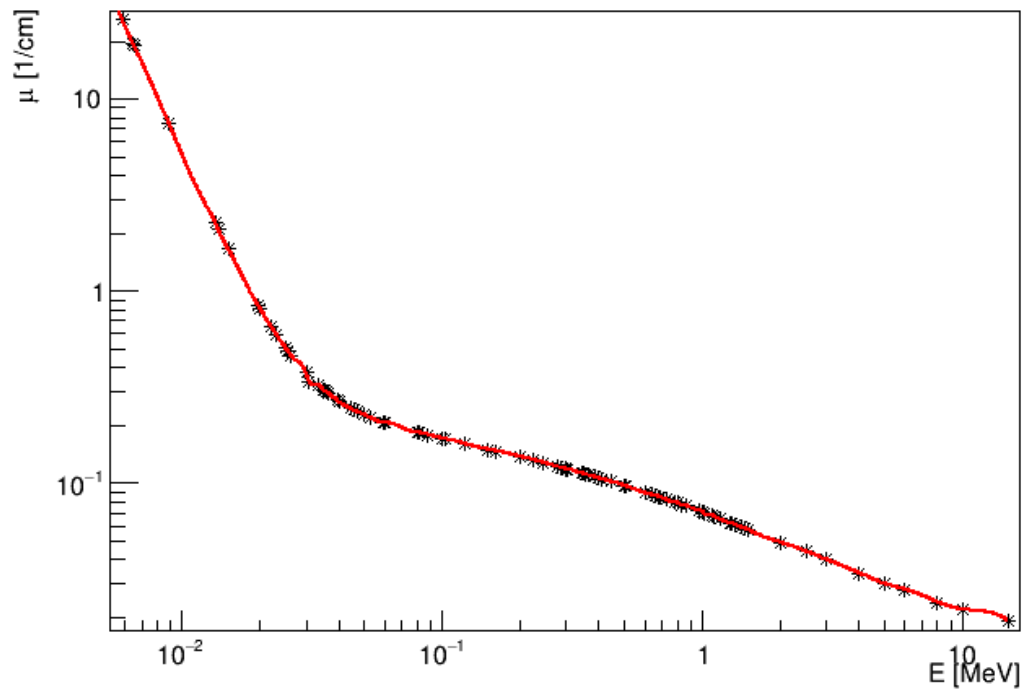


Figure 9: Linear attenuation coefficient for bones with linear interpolation.

## 5 Gamma quantum absorption for annihilation at the center of the brain

Probability that gamma quantum with energy  $E$  is not absorbed and pass through the head, according to the equation 12, is equal to:

$$P = e^{-\mu_B(E)d_B}. \quad (18)$$

The simplest case of gamma quanta absorption is decay in the center of the brain. Due to the assumption that the brain is spherical, a distance of each gamma quanta in the brain is the same and is equal to radius of the brain. Value of this radius is calculated from volume of average size of brain from reference [14] and it is equal to:

- for women:  $d_B = 6.53$  cm,
- for men:  $d_B = 6.93$  cm.

In this study, the size of the brain was overestimated and a  $d_B = 7$  cm was assumed for both men and women. The Monte Carlo simulation was based on generating 1,000,000 decays, both p-Ps and o-Ps, and checking whether a given quantum has been absorbed with probability given in equation 18. Then those that had not been absorbed and had gone out of the head were counted. For two gamma from p-Ps total probability equals to:

$$P_{total} = P_1P_2, \quad (19)$$

for three gamma from o-Ps equals to:

$$P_{total} = P_1P_2P_3, \quad (20)$$

where

$$P_1 = e^{-\mu(E_1)d_B}, \quad P_2 = e^{-\mu(E_2)d_B}, \quad P_3 = e^{-\mu(E_3)d_B}, \quad (21)$$

for two gamma quanta from p-Ps decay the energy of each photon is always equal  $E = 511$  keV and value of attenuation coefficients are given in equations 16, 17.

For the case with skull first I checked absorption in the brain, then I calculated absorption in the skull which is also given by formula 18, but now distance  $d$  is equal to the value of thickness of the skull. The average thickness of the skull bone  $d_S$  determined from the data given in the reference [15]:

- for women:  $d_S = 6.51$  mm,
- for men:  $d_S = 6.54$  mm.

In this study, the thickness of the skull bones was overestimated and the distance in the skull was assumed  $d_S = 6.55$  mm for both men and women. So the probability of getting out of the head, that is, passing through the brain and skull, for one gamma quanta with energy  $E$  is given by the formula:

$$P = e^{-\mu_B(E)d_B} e^{-\mu_S(E)d_S}. \quad (22)$$

To check that Monte Carlo simulations are correct, it is possible to do analytical calculations by the above formulas for one energy. The correctness can also be checked by considering non-physical situations and the comparison of these results obtained for these situations using the Monte Carlo method and analytical calculations. This situation assumes that scattering is not included in attenuation coefficient. Hence the scatter must be taken into account in formula for total probability. Probability for scattering  $P_s$  is equal to:

$$P_s = 1 - P, \quad (23)$$

where  $P$  denotes probability for passing through the brain and skull. The number of scattered photons in one event can be one, two or three (for o-Ps). There is also a possibility that no gamma quanta will get scattered. If the photon has scattered, it is assumed that there is no chance of leaving the material. Total probabilities for each cases are shown in table 1.

**Table 1:** Formulas for total probabilities for non-physical cases.

Scattered photons	Total probability for p-Ps	Total probability for o-Ps
None	$P_1 P_2$	$P_1 P_2 P_3$
One	$(1 - P_1)P_2 + P_1(1 - P_2)$	$(1 - P_1)P_2 P_3 + P_1(1 - P_2)P_3 + P_1 P_2(1 - P_3)$
Two	$(1 - P_1)(1 - P_2)$	$(1 - P_1)(1 - P_2)P_3 + (1 - P_1)P_2(1 - P_3) + P_1(1 - P_2)(1 - P_3)$
Three	-	$(1 - P_1)(1 - P_2)(1 - P_3)$

## 5.1 Results

Percent of non-absorbed gamma quanta in the brain, from simulations for brain, is equal to:

- $26.10 \pm 0.05$  % for para-positronium,
- $8.40 \pm 0.03$  % for ortho-positronium,

and for brain with skull:

- $20.84 \pm 0.05$  % for para-positronium,
- $5.46 \pm 0.02$  % for ortho-positronium.

Distribution of energy of non-absorbed photons is shown in Figure 10 for brain and Figure 12 for brain with skull. Comparing them with the distribution of energy of photons, immediately after the decay (Figure 6), it can be seen empty areas around 500 keV. It is because when one or two gamma quanta from o-Ps decay have energy close to 500 keV it means that third gamma has little energy and is more strongly absorbed in the head. Therefore, the absorption of gamma quanta with this small energy is greatest. The closer to  $E = 340$  keV, the less gamma quanta are absorbed. When one photon has energy close to  $E = 340$  keV the other two quanta probably have similar energy and all of photons from this decay have the same probability of passing through the head. All three gamma quanta can then reach the detector as opposed to when one or two quanta are absorbed. In the case of absorption of one or two of the gamma quanta,  $3\gamma$  imaging is ineffective. Fractions of absorbed events is shown in tables 2, 4 (for gamma quanta from p-Ps decay) and tables 3, 5 (for gamma quanta from o-Ps decay). In the tables there are also results of simulations and analytical calculation for non-physical cases. The results of simulations are presented as:

$$\frac{N_p}{N_s} \pm \frac{\sqrt{N_p}}{N_s}, \quad (24)$$

where  $N_p$  denotes number of events for which all gamma quanta came out of the head,  $N_s$  denotes number of simulated events. The results obtained from the simulations for all scattering cases agree with the analytical calculations to within a several standard deviation. Large uncertainty values for energy  $E = 340$  keV result from the fact that Monte Carlo simulation for this energy is a range of energy from 337 keV to 343 keV and from 1,000,000 simulated photons only 164 have energy from this range. This is a small number to have good statistics.

Ratio of energy distribution non-absorbed photons (Figures 10, 12) to energy distribution of all photons from ortho-positronium decay (Figure 6) is shown in Figures 11, 13.

**Table 2:** Fraction of non-absorbed gamma quanta for the different scattering. Case: para-positronium and brain.

Scattered photons	Monte Carlo [%]	Analytical calculations [%]
None	$26.10 \pm 0.05$	25.9
One	$49.97 \pm 0.01$	50.0
Two	$23.96 \pm 0.05$	24.1

**Table 3:** Fraction of non-absorbed gamma quanta for the different scattering. Case: ortho-positronium and brain.

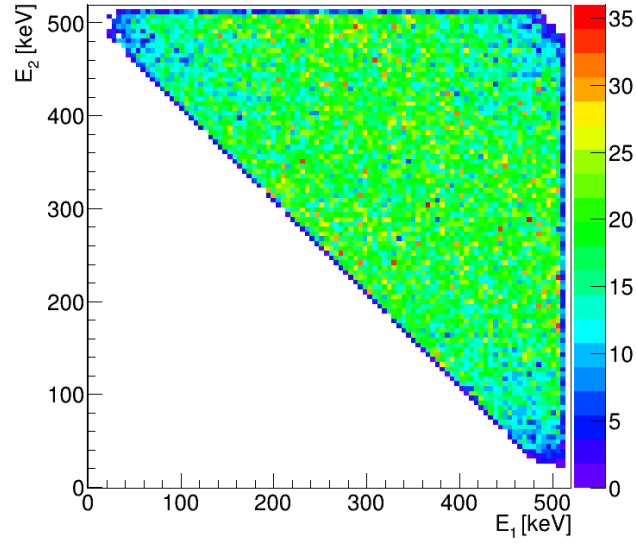
Scattered photons	Monte Carlo for all energies [%]	Monte Carlo for $E = 340$ keV [%]	Analytical calculations for $E = 340$ keV [%]
None	$8.40 \pm 0.03$	$11.0 \pm 2.6$	9.5
One	$32.99 \pm 0.06$	$42.7 \pm 8.8$	33.9
Two	$41.68 \pm 0.07$	$45.7 \pm 9.1$	40.5
Three	$17.05 \pm 0.04$	$16.5 \pm 3.2$	16.1

**Table 4:** Fraction of non-absorbed gamma quanta for the different scattering. Case: para-positronium and brain with skull.

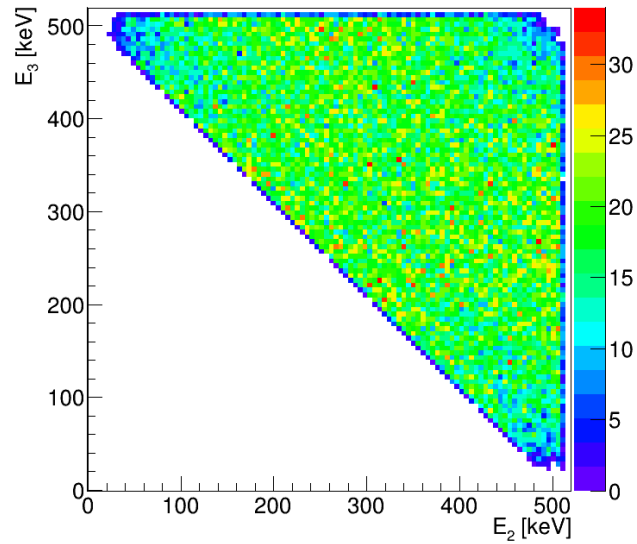
Scattered photons	Monte Carlo [%]	Analytical calculations [%]
None	$20.84 \pm 0.05$	21.0
One	$49.75 \pm 0.01$	49.7
Two	$29.54 \pm 0.05$	29.3

**Table 5:** Fraction of non-absorbed gamma quanta for the different scattering. Case: ortho-positronium and brain with skull.

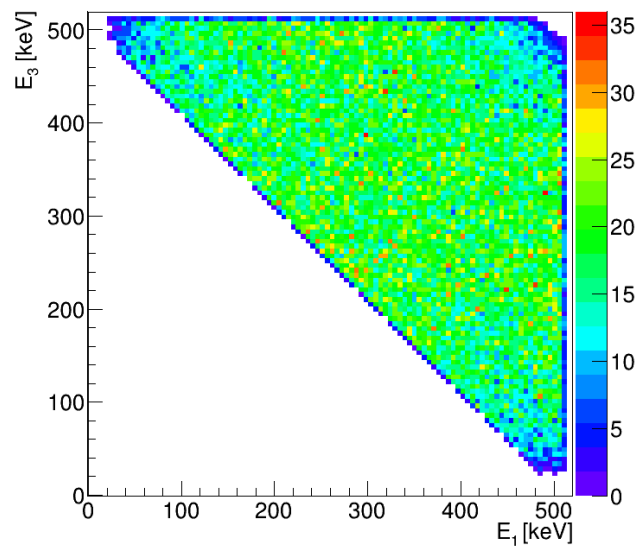
Scattered photons	Monte Carlo for all energies [%]	Monte Carlo for $E = 340$ keV [%]	Analytical calculations for $E = 340$ keV [%]
None	$5.46 \pm 0.02$	$6.1 \pm 1.9$	6.4
One	$27.43 \pm 0.09$	$27.4 \pm 7.1$	28.7
Two	$44.14 \pm 0.12$	$39.6 \pm 8.5$	43.2
Three	$22.88 \pm 0.05$	$20.7 \pm 3.6$	21.7



(a) Distribution of  $E_1$  and  $E_2$ .

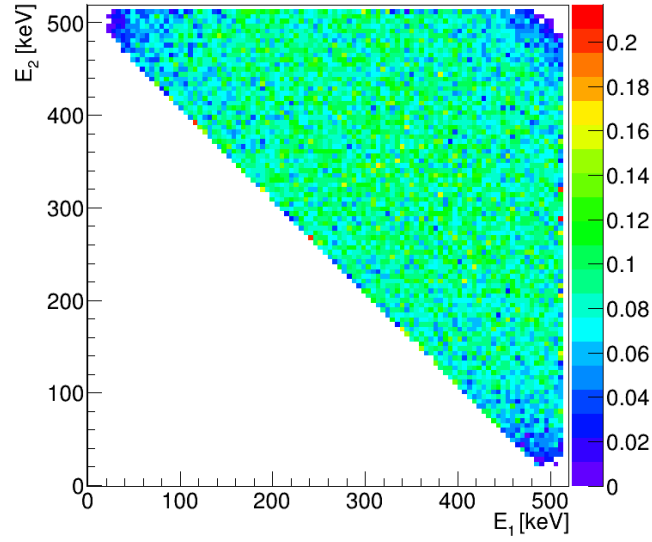


(b) Distribution of  $E_2$  and  $E_3$ .

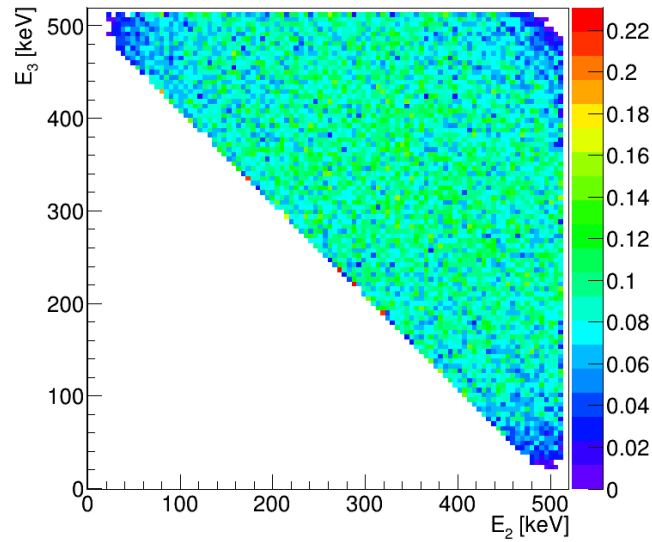


(c) Distribution of  $E_1$  and  $E_3$ .

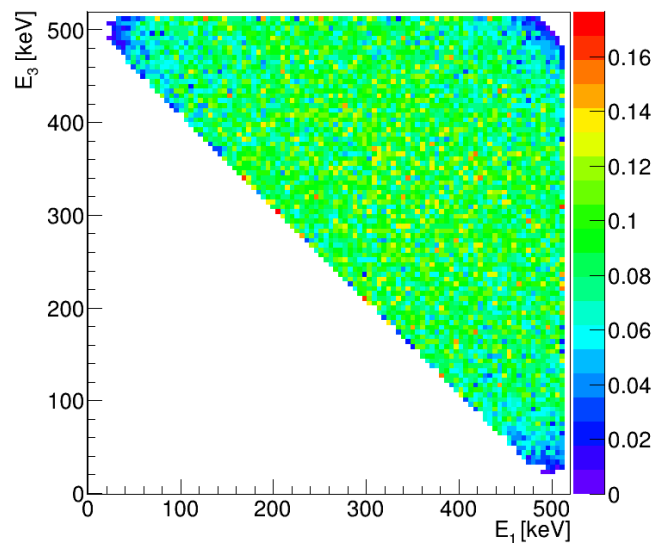
**Figure 10:** Distribution of energy of gamma quanta from ortho-positronium decay after passing through the brain.



(a) Distribution of  $E_1$  and  $E_2$ .

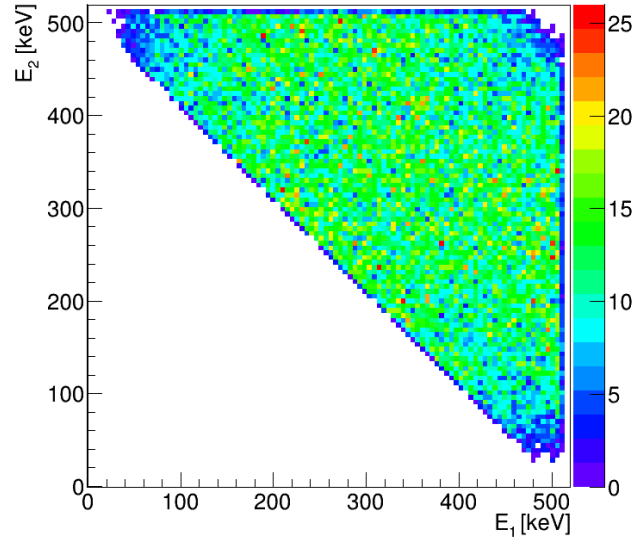


(b) Distribution of  $E_2$  and  $E_3$ .

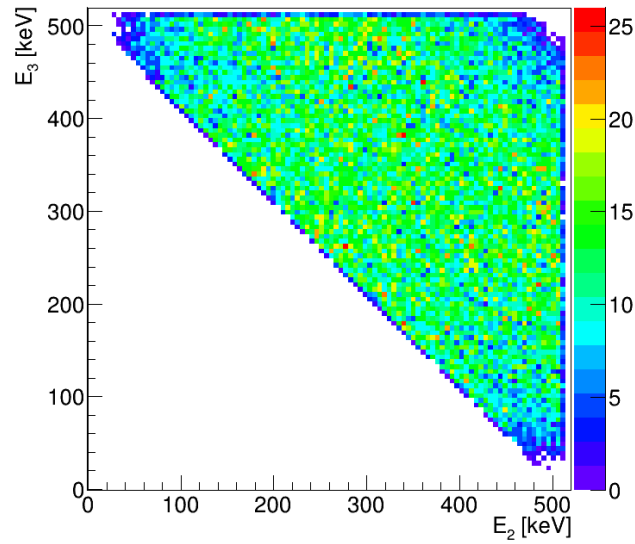


(c) Distribution of  $E_1$  and  $E_3$ .

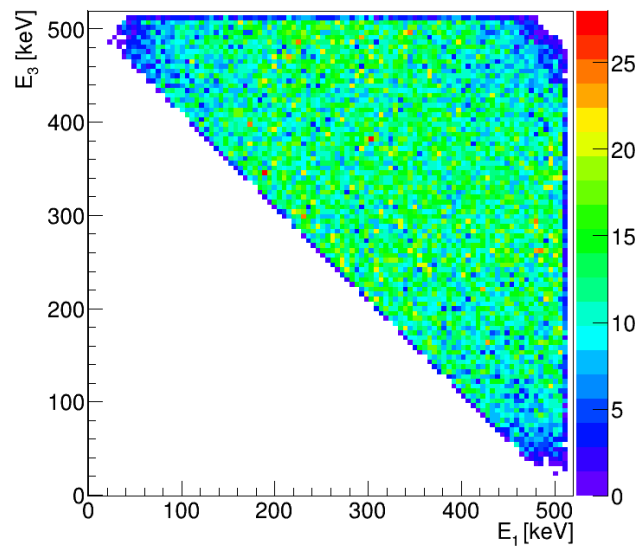
**Figure 11:** Distribution of the ratio of gamma quanta from ortho-positronium decay after passing through the brain (Figure 10) and distribution of energy of all gamma quanta from ortho-positronium decay (Figure 6).



(a) Distribution of  $E_1$  and  $E_2$ .

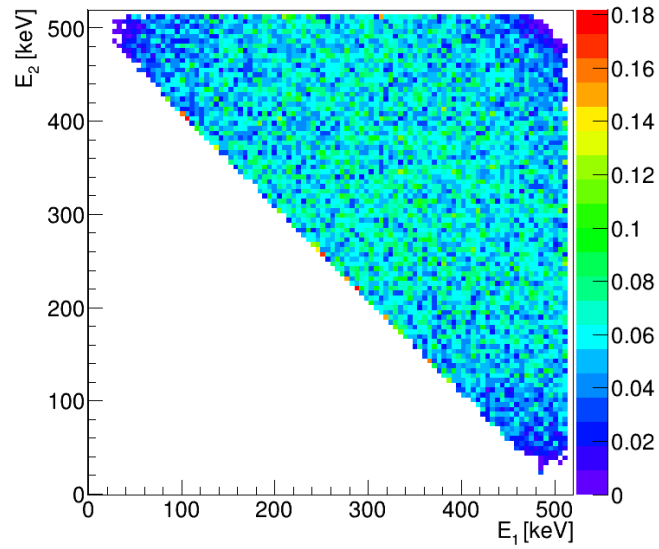


(b) Distribution of  $E_2$  and  $E_3$ .

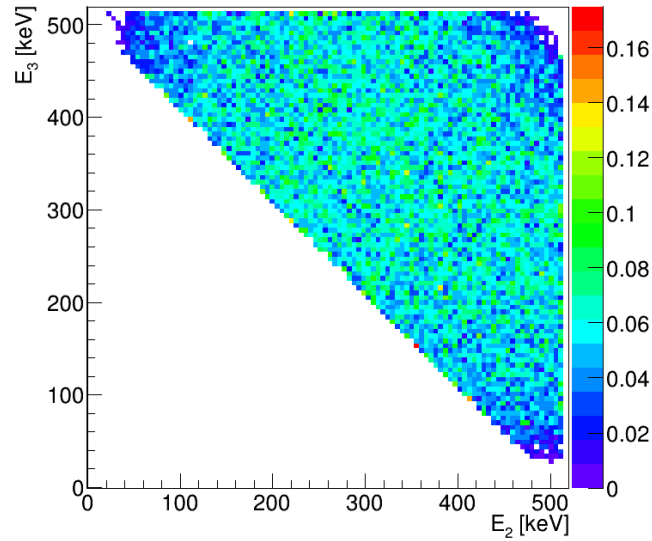


(c) Distribution of  $E_1$  and  $E_3$ .

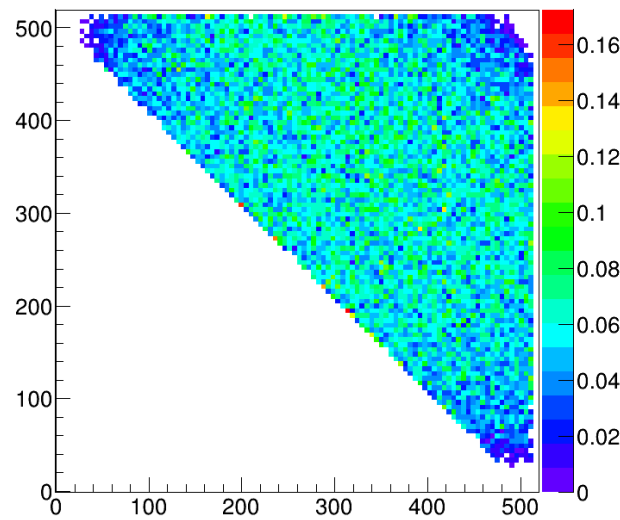
**Figure 12:** Distribution of energy of gamma quanta from ortho-positronium decay after passing through the brain and skull.



(a) Distribution of  $E_1$  and  $E_2$ .



(b) Distribution of  $E_2$  and  $E_3$ .



(c) Distribution of  $E_1$  and  $E_3$ .

**Figure 13:** Distribution of the ratio of gamma quanta from ortho-positronium decay after passing through the brain (Figure 12) and distribution of energy of all gamma quanta from ortho-positronium decay (Figure 6).

## 6 Gamma quantum absorption for annihilation in a random place in the brain

The next consider case is situation when positronium decay is in the random place in the brain. I homogeneously draw annihilation point in the brain. Using previous assumption that the brain is a sphere I generate homogeneously points  $\vec{\sigma} = (x, y, z)$  in the sphere. First I do simulations for 1,000,000 points to check, if sphere is really homogeneously distributed. The coordinates of the points are determined in a spherical system:

$$x(r, \theta, \phi) = r \sin \theta \cos \phi, \quad (25)$$

$$y(r, \theta, \phi) = r \sin \theta \sin \phi, \quad (26)$$

$$z(r, \theta, \phi) = r \cos \theta. \quad (27)$$

Jacobian of this transformation is equal:

$$\mathbf{J} = r^2 \sin \theta = A \frac{dr^3 d \cos \theta d\phi}{dr d\theta d\phi}, \quad (28)$$

with a constant A. Hence I draw  $r^3$ ,  $\cos \theta$ ,  $\phi$  by function *TRandom2()* with homogeneous distribution. Histogram of distribution points in the sphere is shown in Figure 14(a). Cross section XY of sphere is in Figure 14(b). The slice thickness is equal 5 bins.

According to the formula describing the absorption (equation 12) quanta attenuation depends on distance passed. When point of annihilation is not in the center of the brain distance in the head is different for each place (Figure 15).

Knowing the direction in which the quantum is going  $\hat{u}$ , decay place  $\vec{\sigma}$ , radius  $r$  and center of the sphere  $\vec{m}$  one can write equations for sphere [16]:

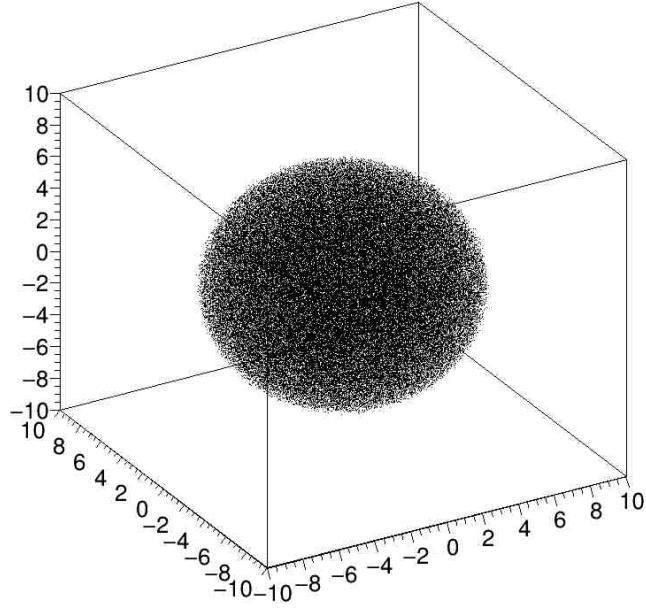
$$\|\vec{x} - \vec{m}\| = r^2, \quad (29)$$

and for line

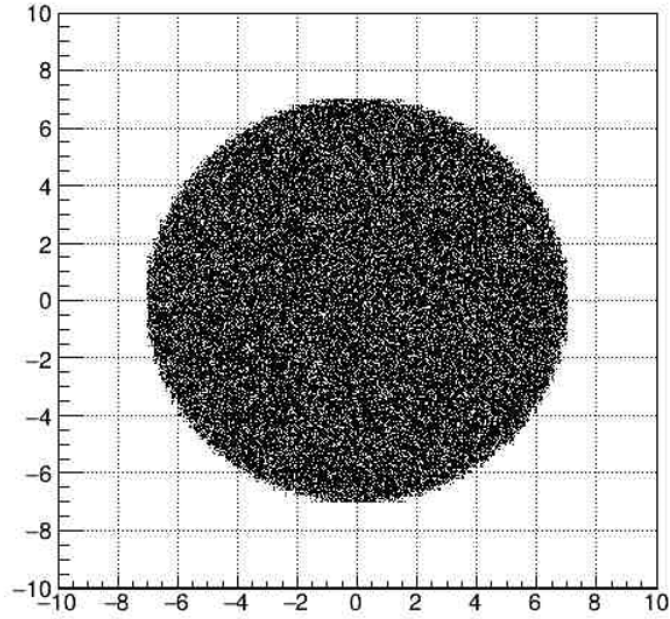
$$\vec{x} = \vec{\sigma} + d\hat{u}, \quad (30)$$

which is a line through the decay point and two points on the sphere. Combining the two equations above:

$$\|\vec{\sigma} + d\hat{u} - \vec{m}\| = r^2, \quad (31)$$



(a) Histogram of distributions points in the sphere.



(b) Cross section XY.

**Figure 14:** Homogeneous distribution of points in the sphere.

one can find the points of intersection of the line with the sphere:

$$d = -2[\hat{u} \cdot (\vec{\sigma} - \vec{m})] \pm \sqrt{2[\hat{u} \cdot (\vec{\sigma} - \vec{m})]^2 - 4\|\hat{u}\|^2(\|\vec{\sigma} - \vec{m}\|^2 - r^2)}. \quad (32)$$

For  $\|\hat{u}\|^2 = 1$  and  $\vec{m} = (0, 0, 0)$ :

$$d = -\hat{u} \cdot \vec{\sigma} \pm \sqrt{\Delta}, \quad (33)$$

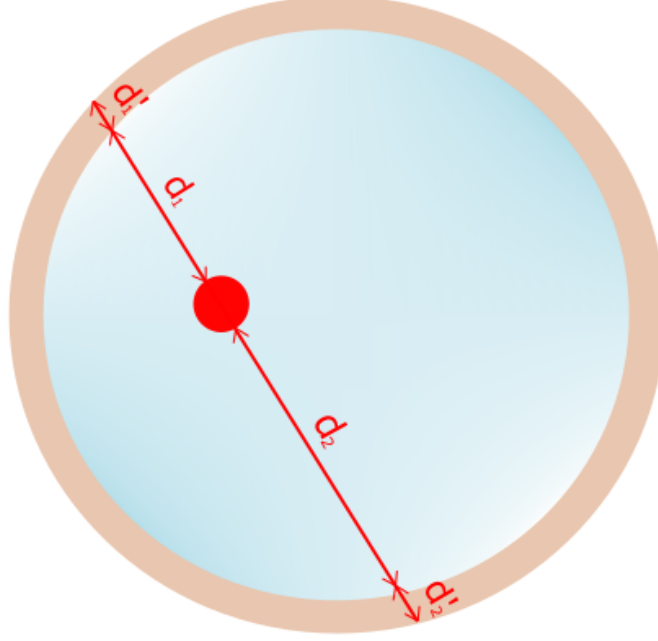


**Figure 15:**  $d_1, d_2$  are the distances in the brain,  $d'_1, d'_2$  are the distances in the skull.

where

$$\Delta = (\hat{u} \cdot \vec{\sigma})^2 - (|\vec{\sigma}|^2 - r^2). \quad (34)$$

When decay is into two photons absolute values for both solutions (equation 33) are distances which photons may pass in the head, but direction of quanta is determined by unit vector  $\vec{u}$ , which is selected in homogeneous sphere (it is described at the begin of this chapter). For three photons directions  $\vec{u}$  are known thanks to o-Ps decay simulations (chapter 4). Vector  $\vec{u}$  is the unit momentum vector. It determines which solution to  $d$  (equation 33) is equal to the path taken by the quantum in the head. For this purpose an auxiliary vector  $\vec{v}$  can be determined. It is a vector between point of annihilation  $\vec{\sigma}$  to one of the solution  $d_1$  from equation 33. The next step is calculating cosine of angle between them:

$$\cos \alpha = \frac{\vec{v} \cdot \vec{u}}{|\vec{v}||\vec{u}|}. \quad (35)$$

If  $\cos \alpha = 1$  it means that, the vector  $\vec{v}$  has the same direction like vector  $\vec{u}$  because angle between them is equal to 0 and  $d_1$  is the true distance. If  $\cos \alpha \neq 1$  second solution  $d_2$  is true.

The distances of the gamma quanta in the skull  $d'_1, d'_2$  can be calculated in the same way as for the brain. One difference is the radius of the sphere, for the brain it is  $d_B = 7$  cm, and for the brain with it is  $d_{(B+S)} = 7.65$  cm, because it is the radius of the brain plus the thickness of the skull. The path in the skull  $d'_S$  is equal to the solutions from the equation 33 for the brain and the skull  $d_S$  minus the solution for the brain  $d_B$ .

Percent of events with non-absorbed gamma quanta depends on the place of decay. It is exponential dependence on attenuation coefficient and distance, which is different for each place. Sphere in which I draw annihilation point is homogeneous, so this dependence can be presented as the amount of non-absorbed photons and distance  $d_o$  from the center of the brain to point  $\vec{o}$ . Distance  $d_o$  is calculated using formula:

$$d_o = \sqrt{x^2 + y^2 + z^2}. \quad (36)$$

This dependence is true for assumption that products of positronium decay are distributed isotropically both para- and ortho-positronium. Plots for each cases (para- and ortho-positronium, brain and brain with skull) are showed below (Figures 16,17, 18, 19). The number of points on plots is 120 in all cases.

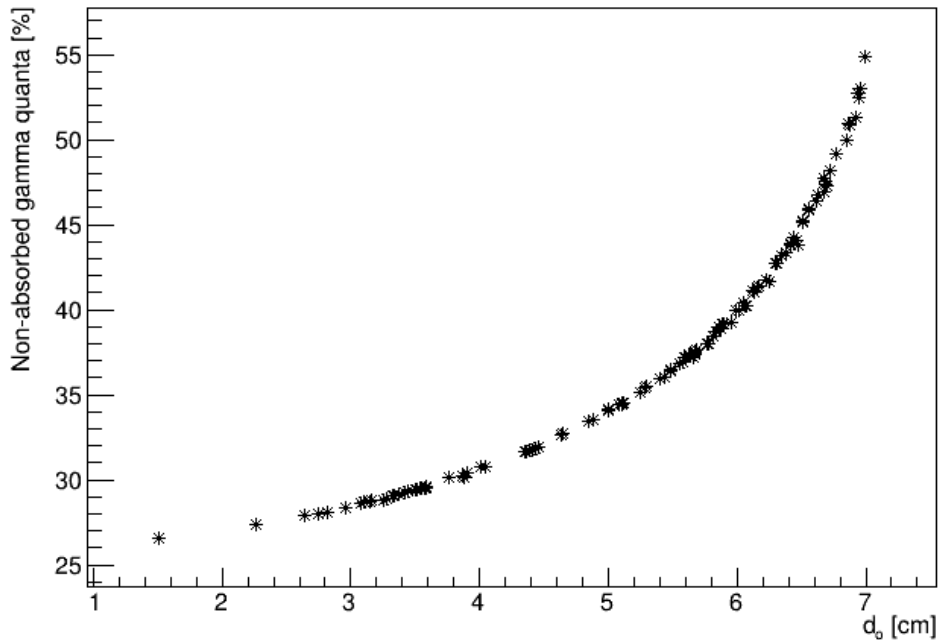


**Figure 16:** Dependence of percent of events with non-absorbed photons on place of annihilation (distance  $d_o$  from the center of the brain to point  $\vec{o}$ ). Case: para-positronium and brain.

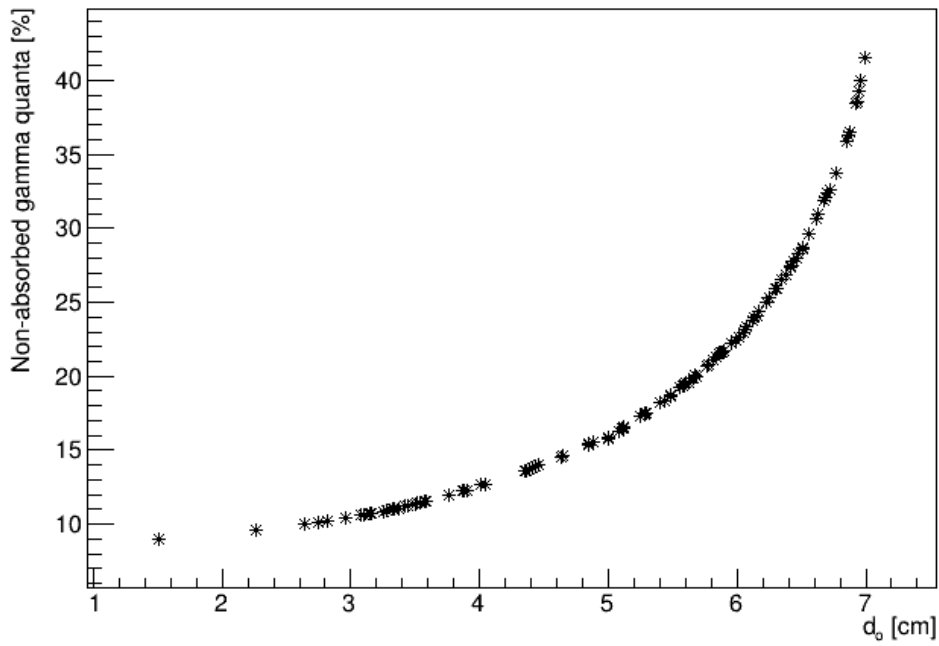


**Figure 17:** Dependence of percent of events with non-absorbed photons on place of annihilation (distance  $d_o$  from the center of the brain to point  $\vec{o}$ ). Case: ortho-positronium and brain.

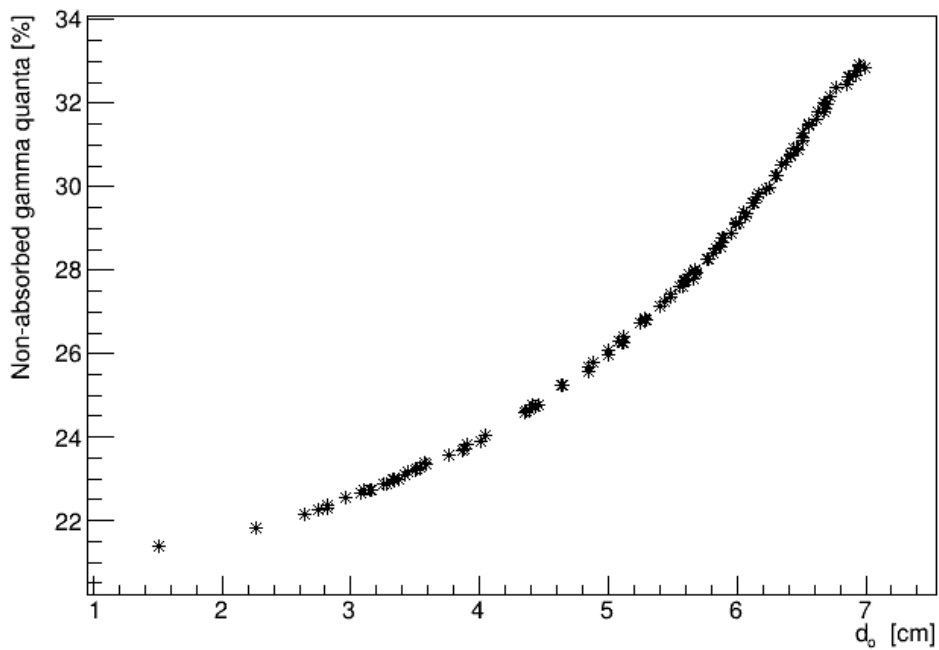


**Figure 18:** Dependence of percent of events with non-absorbed photons on place of annihilation (distance  $d_o$  from the center of the brain to point  $\vec{o}$ ). Case: para-positronium and brain with skull.

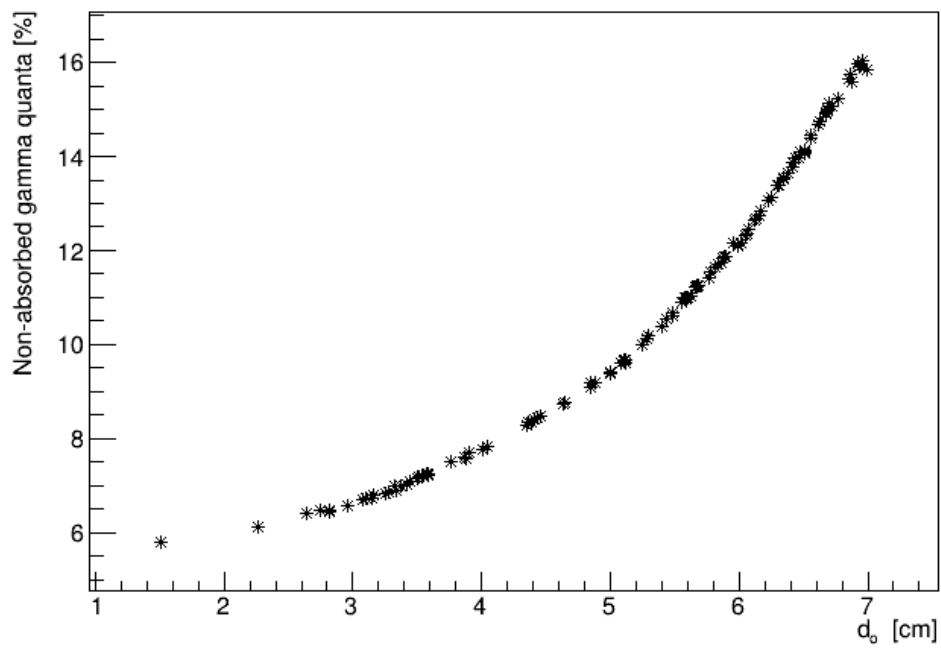


**Figure 19:** Dependence of percent of events with non-absorbed photons on place of annihilation (distance  $d_o$  from the center of the brain to point  $\vec{o}$ ). Case: ortho-positronium and brain with skull.

## 7 $3\gamma/2\gamma$ ratio

### 7.1 Annihilation is at the center of the brain

Simulations made in this study allowed me to calculate  $3\gamma/2\gamma$  ratio  $f_{3\gamma 2\gamma}$  for the brain. It was calculated by formula:

$$f_{3\gamma 2\gamma} = \frac{N_{3\gamma}}{N_{2\gamma}}, \quad (37)$$

where  $N_{3\gamma}$  is the number of o-Ps decay events for which  $3\gamma$  passed through the head and  $N_{2\gamma}$  is the number of p-Ps decay events for which  $2\gamma$  passed through the head. The amount of events for p-Ps and o-Ps was the same (1,000,000).  $3\gamma/2\gamma$  ratio for the results obtained in these studies is shown in table 6. The uncertainties  $\sigma_{f_{3\gamma 2\gamma}}$  of the given values are calculated by the formula:

$$\sigma_{f_{3\gamma 2\gamma}} = \frac{\Delta_{N_{3\gamma}}}{N_{2\gamma}} + \frac{N_{3\gamma} \Delta_{N_{2\gamma}}}{N_{2\gamma}^2}, \quad (38)$$

where  $\Delta_{N_{3\gamma}}$  denotes uncertainty of  $N_{3\gamma}$ ,  $\Delta_{N_{2\gamma}}$  denotes uncertainty of  $N_{2\gamma}$ .

**Table 6:**  $3\gamma/2\gamma$  ratio for Monte Carlo and Analytical calculations for two cases: brain and brain with skull.

Case	Monte Carlo for all energies	Monte Carlo for $3\gamma$ with $E = 340$ keV	Analytical calculations for $3\gamma$ with $E = 340$ keV
Brain	$0.322 \pm 0.002$	$0.50 \pm 0.10$	0.37
Brain with skull	$0.262 \pm 0.002$	$0.46 \pm 0.09$	0.30

### 7.2 Dependence of the ratio $3\gamma/2\gamma$ on the location of the decay

Simulation in this case was the same like in chapter 6. Now plots (Figure 20, 21) show dependence of the  $3\gamma/2\gamma$  ratio on place of annihilation. The number of points on plots is 120 in both cases.

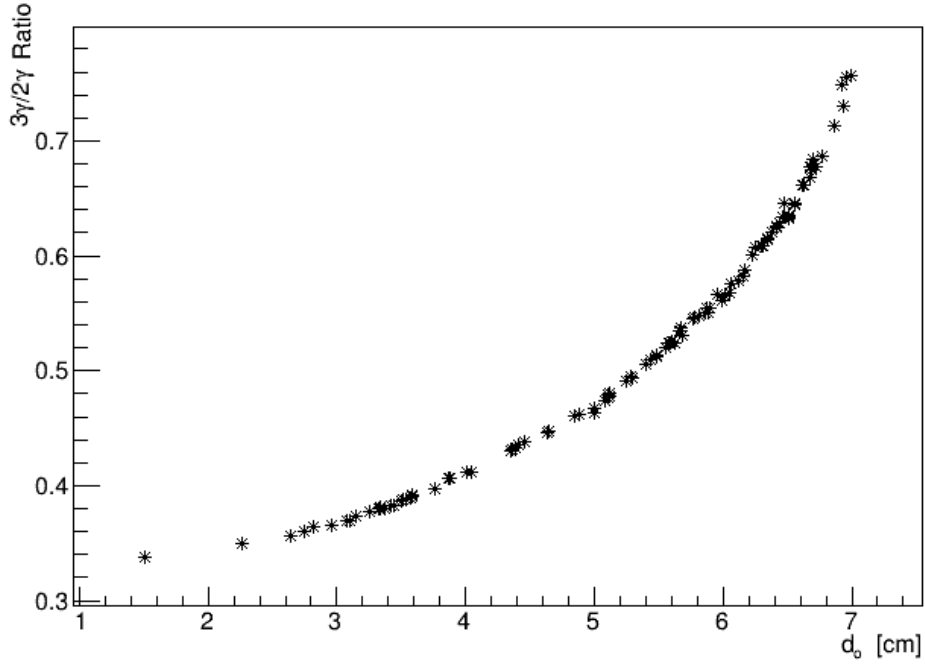


**Figure 20:** Dependence of the  $3\gamma/2\gamma$  ratio on place of annihilation (distance  $d_o$  from the center of the brain to point  $\vec{o}$ ). Case: brain.

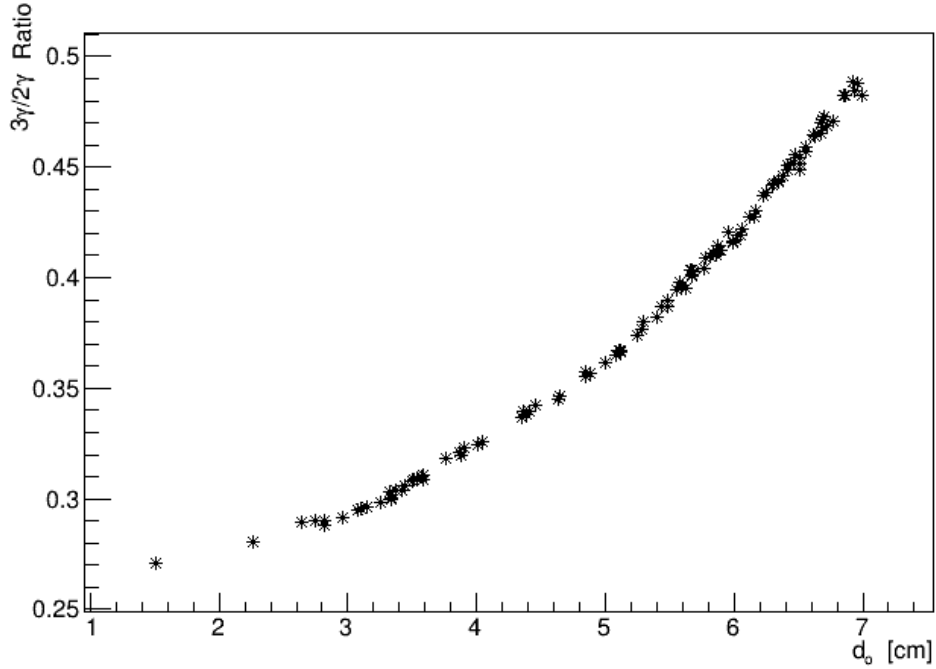


**Figure 21:** Dependence of the  $3\gamma/2\gamma$  ratio on place of annihilation (distance  $d_o$  from the center of the brain to point  $\vec{o}$ ). Case: brain with skull.

## 8 Summary

In this thesis, the absorption in the brain and skull of gamma quanta from decays of positronium determined, which was the main goal of this work. The brain in this study is approximated by a sphere with water, because attenuation coefficient values for soft tissue are similar to attenuation coefficient values for water. Monte Carlo simulations of positronium atom decay and gamma quantum absorption in brain and skull were performed. The absorption depends on the attenuation coefficient and the distance in the material. The coefficients depend on the energy, so for the energy from positronium decay an interpolation was made for the attenuation coefficient values from reference [11], [12]. The dependence of the absorption on the annihilation location, which is drawn in a homogeneous sphere, was also investigated. The fraction of non-absorbed gamma quanta was determined from Monte Carlo simulations and analytical calculations. Non-physical scattering cases were also considered to check the simulation results with the calculations. The results of the percent of events with non-scattered quanta in the head are as follows:  $26.10 \pm 0.05$  % for para-positronium and  $8.40 \pm 0.03$  % for ortho-positronium (absorption in the brain),  $20.84 \pm 0.05$  % for para-positronium,  $5.46 \pm 0.02$ % for ortho-positronium (absorption in the brain and in skull). The results obtained from the Monte Carlo simulation are consistent with the analytical calculations with an accuracy of several standard deviations for all cases. The large uncertainties for the simulation of gamma quanta absorption from ortho-positronium decay for energy  $E = 340$  keV are in fact caused by small statistics - out of 1,000,000 events only 164 quanta had energies in the assumed range from 337 keV to 343 keV. In this thesis the  $3\gamma/2\gamma$  ratio is determined also. The structure of the tissue determines the value of this parameter [2]. The values of the  $3\gamma/2\gamma$  ratio from the simulation are:  $0.322 \pm 0.002$  for absorption in the brain and  $0.262 \pm 0.002$  for absorption in the brain and skull. Simulation results for  $3\gamma/2\gamma$  ratio are also consistent with analytical calculations to within a few standard deviation. The dependence of absorption and  $3\gamma/2\gamma$  ratio on the decay location of the positron atom in the brain was also determined.

## References

- [1] P. Moskal, D. Kisielewska, C. Curceanu et al., "Feasibility study of the positronium imaging with the J-PET tomograph", *Phys. Med. Biol.* **64**:055017 (2019).
- [2] B. Jasińska, P. Moskal, "A New PET Diagnostic Indicator Based on the Ratio of  $3\gamma/2\gamma$  Positron Annihilation", *Acta Phys. Pol. B*, **48**:1577-1582 (2017).
- [3] F. Bray, J. Ferlay, I. Soerjomataram et al., "Global cancer statistics 2018: GLOBOCAN estimates of incidence and mortality worldwide for 36 cancers in 185 countries" *CA: Cancer J. Clin.* **68**:394-424 (2018).
- [4] P. Moskal et al. "Performance assessment of the  $2\gamma$  positronium imaging with the total-body PET scanners", *EJNMMI Phys* **7**:44 (2020).
- [5] A.H. Al-Ramadhan, D.W. Gidley, "New precision measurement of the decay rate of singlet positronium", *Phys. Rev. Lett.* **72**:1632 (1994).
- [6] R.S. Vallery, P.W. Zitzewitz, D.W. Gidley, "Resolution of the Orthopositronium-Lifetime Puzzle", *Phys. Rev. Lett.* **90**:203402 (2003).
- [7] L. D. Landau, E. M. Lifshitz, "Quantum mechanics: non-relativistic theory" (3rd ed.) *Pergamon Pr* (1981).
- [8] D. Kamińska, A Gajos, E. Czerwiński, et al., "A feasibility study of ortho-positronium decays measurement with the J-PET scanner based on plastic scintillators", *Eur. Phys. J. C*, **76**:445 (2016).
- [9] J. Chhokar, "Simulation of Positronium Decays in View of Charge Conjugation Symmetry Test with the J-PET Detector" *Acta Physica Polonica A* **137**:134-136, (2020).
- [10] A. Strzałkowski, "Wstęp do fizyki jądra atomowego" *Państwowe Wydawnictwo Naukowe* (1969).
- [11] E. Şakar, Ö. Fırat Özpolat, B. Alım et al., Phy-X / PSD: Development of a user friendly online software for calculation of parameters relevant to radiation shielding and dosimetry, *Radiat. Phys. Chem.* **166** (2020).
- [12] J. Hubbell, S. Seltzer, "Tables of X-Ray Mass Attenuation Coefficients and Mass Energy-Absorption Coefficients 1 keV to 20 MeV for Elements  $Z = 1$  to 92 and 48 Additional Substances of Dosimetric Interest", *Radiation Physics Division, NIST* (1995).
- [13] E.K., Nyer, Jr., P. Fierro, "The Water Encyclopedia: Hydrologic Data and Internet Resources" (3rd ed.), *CRC Press* (2007).

- [14] C. Del, T. Craneal, P. Bayat, et al., "Correlation of Skull Size and Brain Volume, with Age, Weight, Height and Body Mass Index of Arak Medical Sciences Students", *J. Morphol.* **30**:157-161 (2012).
- [15] F. Farzana, B. Shah S. Shadad et al., "Computed tomographic scanning measurement of skull bone thickness: a single center study", *Int. J. Med. Sci.* **6**:913 (2018).
- [16] David H. Eberly, "3D game engine design: a practical approach to real-time computer graphics" (2nd ed.), *Morgan Kaufmann* (2006).